

# Reliability Meta-modelling of Power Components

Stoyan Stoyanov<sup>1)</sup>, Tim Tilford<sup>1)</sup>, Yaochun Shen<sup>2)</sup>, Yihua Hu<sup>3)</sup>

<sup>1)</sup> School of Computing and Mathematical Sciences, University of Greenwich, London, UK

<sup>2)</sup> Department of Electrical Engineering and Electronics, University of Liverpool, Liverpool, UK

<sup>3)</sup> Department of Engineering, Kings College London, London, UK Country

Email: [s.stoyanov@greenwich.ac.uk](mailto:s.stoyanov@greenwich.ac.uk) ORCID: [0000-0001-6091-1226](https://orcid.org/0000-0001-6091-1226)

**Abstract**—Finite element (FE) modelling integrated with lifetime prediction models is an attractive and powerful approach for predicting and improving the thermal fatigue reliability of power electronic components and modules subjected to temperature cycling loads. The challenge with the FE-based modelling approach is the model development effort, device characterisation data requirements and the computational cost of the high-fidelity simulation. This paper presents a modelling methodology for developing fast and user-friendly damage prediction models for power components that benefit from the combined deployment of meta-modelling and machine learning (ML), using physics-informed damage data. The main attribute of the meta-modelling framework is the FE-like mapping of the spatial distribution of the thermal fatigue damage parameter in the local domain of the failure site. The thermal fatigue predictions for the planar solder interconnection layer in a conventional wire-bonded, Si-based Insulated-Gate Bipolar Transistor (IGBT) power electronic module (PEM) are demonstrated using the proposed methodology under parameterised thermal cycling load. The results show that the metamodel with location-dependent model parameters can retain the accuracy of damage predictions obtained with the full-order FE simulations and can accurately inform on the damage spatial distribution in the solder layer. The metamodel is found to have superior performance compared to a unified Neural Network model with the same spatial damage prediction attribute.

**Keywords** — Power components, IGBT, reliability, solder interconnects, metamodels, thermal fatigue, damage, Machine Learning

## I. INTRODUCTION

Power electronic components are used to convert and control electrical energy, and therefore they are widely used in many applications ranging from renewable energy (e.g. solar and wind power) and smart grids to electric vehicles and industrial drives to consumer appliances and chargers of electronic devices [1]. One of the main driving forces of the power electronics technology along with cost, volume, weight, and functionality is reliability. The reliability of power electronic packages is a serious concern and a major challenge for the end-users of power electronic components and modules because high-reliability requirements mark almost any application of power electronics [2,3]. Despite the significant body of reliability-focused research and studies in the public domain, on technology, design, test and simulation, the informed deployment of packaged power electronic devices in different applications remains a challenging task. To assure the required reliability of power components under application-specific load conditions, end-users must carry out

time-consuming and costly activities, e.g. substantial physical and reliability tests, often complemented with complex high-fidelity physics-based simulations, to characterise, evaluate and assure their reliability performance [4,5].

The deployment of reliability assessment approaches that rely on simulating the physics-of-failure in the power electronic components is increasingly recognised as a powerful and efficient strategy to gain insights into the reliability performance and lifetime of power electronics [6]. While several failure modes and mechanisms at the package level can occur and thus have a direct impact on reliability, it is the thermal fatigue damage which is of prime concern [5]. Temperature cycling loads make the die attachment and interconnection layers (commonly solder) and the wire bonds susceptible to failure under modes such as interfacial cracking and lift-off, receptively. Both solder interconnection layer damage modelling, for example [7,8], and wire bond lift-off failure simulations, for example [9,10], have received extensive attention in power electronics reliability studies.

The design and manufacture of a power electronic component is a challenging task that requires careful consideration of the device's performance in the electrical, thermal, and mechanical domains. The functional performance and characteristics are regarded as being the most critical from an end-user point of view and therefore are comprehensively detailed in the manufacturer's component datasheets. However, other characterisation data (for example internal package construction, geometric dimensions, materials, and material properties) is typically not included in the manufacturers' technical datasheets because of Intellectual Property (IP) and know-how protection reasons and considerations.

Although power electronic components are increasingly designed to deliver an adequate reliability performance, these parts are still designed and manufactured by large in a non-specific application manner. The current position is that any deployment of physics-of-failure modelling requires the end-user to undertake a full characterisation of the power component or module of interest, deploying different experimental characterisation techniques, to gather the required data on the device. This data can then support the respective damage mechanics model development, e.g. finite elements based, that can be used to predict the damage induced in the assembly materials under the user-defined application or accelerated life test load condition. High-fidelity model development and simulation on its own is a challenging task as it needs specialised modelling skillsets and software and is also time-consuming to develop and run.

To improve on this current position, alternative modelling approaches are needed to offer simple, fast-to-run, and

---

The work is supported by the Engineering and Physical Sciences Research Council (EPSRC), U.K., through project grant EP/R004390/1 and the multi-partner grants EP/W006642/1, EP/W006405/1, EP/W006308/1.

accurate models that can be deployed with ease by the end-users, for example in line with the surrogate modelling strategies in [11-14].

In this paper, a reliability metamodeling methodology for power electronics modules that allows for the assessment of the damage due to application loads without the need for comprehensive data characterisations, specialised simulation software and specialised modelling skills is proposed and demonstrated. The novel attribute of the approach which makes it useful and deployable, apart from the superior computational efficiency, is the enhanced level of fidelity, enabling the spatial distribution prediction of the damage parameter in the power assembly materials at the local failure site. The proposed metamodels can thus benefit the deployment of different lifetime models available in the public domain which by large are not standardised and can require as input damage spatial distribution information.

## II. META-MODELLING METHODOLOGY

### A. Metamodeling of Damage Spatial Distribution using Multi-Quadratic Functions

Traditionally, the Response Surface (RS) approach in engineering has been considered and used in the design-of-experiments (DOE) investigations, and to support design-for-reliability studies with a clear focus on the design exploration and optimisation of physical systems [15]. Most RS developments and applications remained limited to the construction of approximation- and interpolation-based surrogate models that encompassed the relationship between design parameters considered for improvement and a physical variable that needs to be predicted. However, the methodology has also the potential, not realised yet, to be utilised for the problem of product intellectual property (IP) protection while at the same time allowing for an adequate fidelity of the modelling prediction. In the context of this work, the model-predicted parameter is the material damage accumulation in the failure site of the power device package under thermal fatigue loads of a specific application, and the increased level of fidelity of the metamodel is in the ability to predict the spatial distribution of the damage parameter over a user-defined subspace linked to the failure site.

The proposed computational methodology involves several steps, formulated here for the problem of modelling and predicting the thermal fatigue damage in the planar solder interconnection layer of a conventional IGBT wire-bonded Si chip power electronic module structure. Each step and the modelling data/results flow between the steps are fully automated. The automation of the steps is a key requirement to enable the practical realisation of the approach. The targeted metamodel structure takes as inputs the temperature load parameters and the spatial coordinates of locations that define the local domain of the failure site, and the model prediction is for energy-based damage metric for the solder material. Most commonly, the accumulated deformation energy per cycle (inelastic strain energy density, or plastic work, i.e. the area enclosed by the hysteresis loop) is used as a damage parameter and input in Morrow's type of fatigue law to predict the cycles to failure  $N_f$  [16,17]:

$$N_f = A(\Delta W)^{-B} \quad (1)$$

where  $A$  and  $B$  empirically derived constants and  $\Delta W$  is accumulated deformation energy per cycle, commonly derived as a volume-weighted average at the crack location.

The workflow of the proposed methodology is as follows:

*Step 1:* The PEM of interest is fully characterised (internal layout, geometric dimensions, bill of materials, material properties and non-linear constitutive laws). The temperature cycling load condition is parametrised and the limits of the design space for the load, informed by the application/qualification test requirement for the PEM, are specified.

*Step 2:* For the given PEM structure, a fully scripted high-fidelity non-linear finite element model generation (parametric model) is prepared, and automated design-of-simulations runs (load cases) in the thermal load design space are carried out. The simulation results are physics-informed datasets for the damage (plastic work) at the anticipated failure sites (the solder layer in this instance) as a function of the analysed load cycles. Damage results are extracted and processed in an automated manner and split into datasets for model development (training data) and model validation.

*Step 3:* Deploy a robust multi-quadratic (MQ) metamodel structure to represent the load-damage relationships in the spatial domain of the failure site. The metamodel generation is extended to spatial location predictions through an approach where the MQ metamodel coefficients are made location-dependent. The spatial location points are defined by the spatial coordinates of the FE mesh nodes or mesh elements' centres at the failure site and chosen to allow visualisation of the metamodel predicted damage distribution.

*Sub-step 3.1:* For a given spatial location, construct the respective MQ model using the training data. Validate the model against the validation dataset. Extract the location-dependent model coefficients.

*Sub-step 3.2:* Repeat *Sub-step 3.1* until the metamodel is developed for all spatial locations of interest for the failure site. Use the final model to predict the spatial distribution of material damage under an arbitrary temperature cycle load within the load space.

The workflow of the proposed methodology is schematically outlined with the block diagram given in Fig. 1.

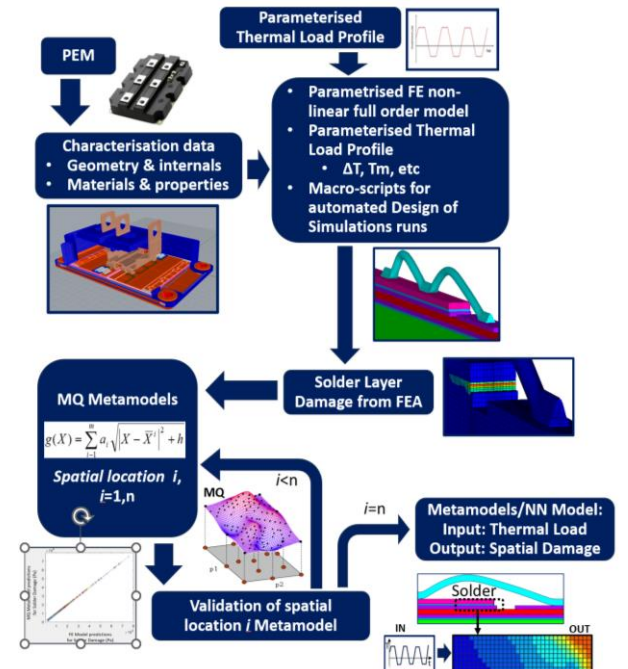


Fig. 1. Methodology for physics-informed multi-quadratic meta modelling.

Underpinned by physics-of-failure data for the PEM solder damage, and locational damage distribution data informed by the FEA analysis, the final metamodel can provide predictions not only for the characteristic damage value of the respective failure mode (i.e. crack of the solder layer) but a much more detailed prediction for the spatial distribution of the damage parameter. The model does not require any other input data (e.g. no geometric and material data) apart from the load condition under which the damage needs to be predicted. The availability of damage spatial distribution is a major advantage because it enables a robust deployment of different lifetime models in the public domain.

### B. Neural Network Model Extension

The availability of physics-informed datasets also supports the use of machine learning (ML) methods for the development of an MQ-equivalent metamodel. Regression type Artificial Neural Network (NN) model structure suits well the data and the task. Unlike the MQ metamodeling approach, the datasets for NN model development are further processed in the form of unified labelled data where the input is specified as a multi-dimensional vector combining both the temperature cycle parameters and the coordinates of the spatial locations. The approach also favours the deployment of an enlarged training dataset which can combine both the prime FE-based data and additional MQ metamodel generated data if the accuracy of the MQ metamodel is acceptable.

## III. DEMONSTRATION CASE STUDY

### A. IGBT Power Module

The power electronic module in this study is a conventional IGBT package as schematically illustrated in Fig. 2. In this architecture, the Si chip (IGBT) is attached to a ceramic substrate such as Alumina ( $\text{Al}_2\text{O}_3$ ) or Aluminium Nitride (AlN). The substrate has copper metallization on both sides that realises the required current circuitry and contact terminals for interconnections and bus bars. The copper metallization layers are formed through direct thermal bonding, giving the name direct bond copper (DBC) substrate. The chip is attached to the DBC substrate by soldering, and similarly, the chip/DBC substrate assembly is attached with a solder layer to the baseplate. The baseplate is typically made of Cu or AlSiC and provides the required structural integrity of the entire PEM package. To allow for enhanced thermal management, most PEM applications deploy a heat sink attached to the baseplate.

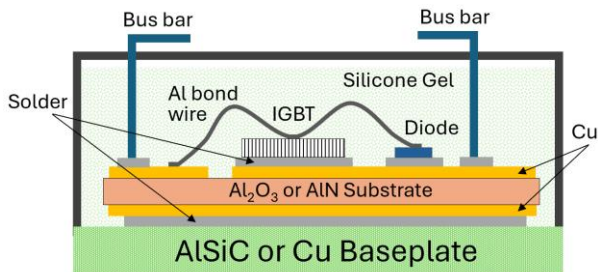


Fig. 2. Schematic of a typical IGBT power module packaging architecture.

### B. Thermo-mechanical Finite Element Model

A 3D FE slice model of the IGBT module is deployed, encompassing a single wire of the device and the complete layered structure through the full thickness of the package. Fig. 3 (top) shows details of the PEM and the 3D slice section as a CAD model, which, in turn, underpins the respective

thermo-mechanical finite element model. The FE model takes advantage of the existing symmetry plane along the 3D slice (X-Z), and hence only half of the demonstrated CAD domain is used and meshed. The backplane of the FE slice model has a coupled-node (DOF Y) boundary condition. Fig. 3 (bottom) also details the finite element mesh and the bill of materials for this PEM. The interconnection material between the Si chip and the copper layer on the AlN substrate is 96.5Sn3.5Ag solder alloy, and similarly between the DBC substrate and the AlSiC baseplate. The thickness of each of the two solder layers is  $100\ \mu\text{m}$ . The visco-plastic material behaviour of solder is modelled with the Anand constitutive law, with model constants for 96.5Sn3.5Ag solder as detailed in [18]. The aluminium wires have a diameter of  $375\ \mu\text{m}$  and are modelled with time-independent bilinear kinematic hardening constitutive law and temperature-dependent yield strength as given in [19].

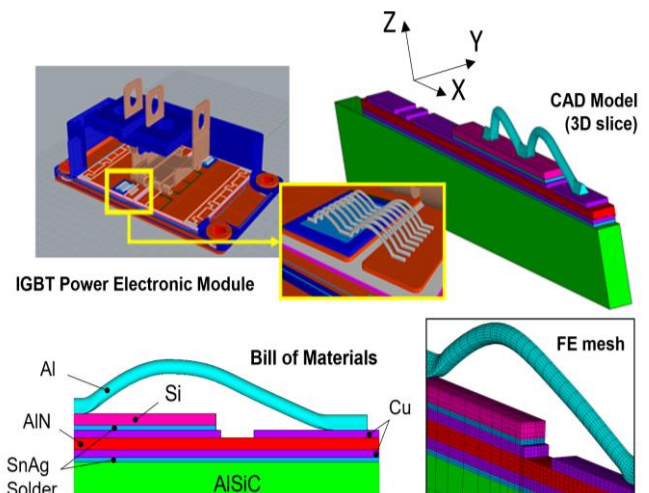


Fig. 3. Topology outline of the power electronic module architecture, with a close view of the IGBT chip and wire bonds and 3D CAD slice model of the device along the full length of the module, capturing a single wire and a full solder layer slice (top), and close view of the FE mesh density at the solder layer level, and annotation labels of the bill of materials (bottom).

The thermo-mechanical simulations are implemented and executed in a fully automated manner using ANSYS APDL FE simulation software command language and macro script functionality. Each thermal cycle profile is evaluated with a separate simulation run for that load case. A temperature cycle load was defined with two parameters: (1) the low-temperature extreme value  $T_{min}$  and the temperature range  $\Delta T$  of the cycle. Although in this study the ramp and dwell times of the cycle are kept fixed for simplifying the demonstration of the methodology, these parameters can be also added to the definition of the cycle load profile. A non-linear transient simulation with the outlined 3D slice model, for a given cycle load, required about 50-65 minutes of high-performance computing run using parallel shared memory with 16 processors on Intel(R) Xeon(R) processor workstation at 2.20 GHz, with 10 cores and 20 logical processors.

Fig. 4 shows an example of FE simulation predictions for the plastic work range per cycle ( $\Delta W$ ) in the solder layer between the Si chip and the DBC substrate. The plastic work accumulated per one temperature cycle with a stabilised hysteresis loop (i.e. inelastic strain energy density per cycle) is a common damage parameter for the thermal fatigue of PEM's planar solder interconnection layers.

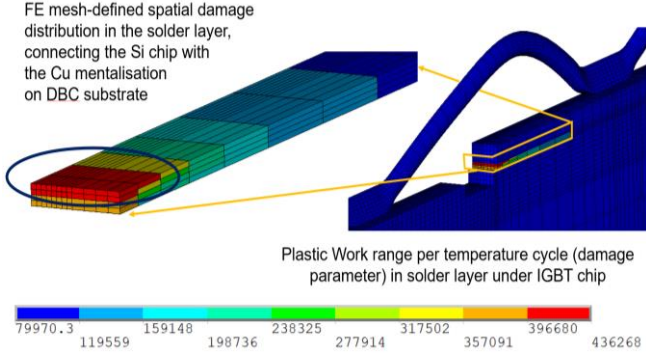


Fig. 4. An example of FE simulation prediction of the plastic work range (damage parameter) magnitude ( $J/m^3$ ) and distribution in the SnAg solder layer of the IGBT power module. The interfacial layer of solder with the chip is the location where the crack is nucleated and starts to propagate.

### C. Datasets for MQ and NN Meta-modelling

The data required for metamodel development is generated with the parameterised thermo-mechanical finite element model and the automated run of 31 load-case simulations. Each analysis is a simulation of the PEM response to a particular passive temperature cyclic load that is defined with the minimum temperature and the magnitude of temperature excursion of the load,  $(T_{min}, \Delta T)_i$ ,  $i = 1, m$ , where in this investigation  $m=31$ . A subset of 21 load cases is used to develop the metamodels (training data), and the remaining 10 load cases are used for validation of the metamodel accuracy against the respective FEA results. The cycling load profiles used to generate the training dataset are defined as follows:

- 6 levels of  $T_{min}$ , from  $-55^\circ C$  to  $145^\circ C$  (step  $40^\circ C$ )
- 6 levels of  $\Delta T$ , from  $40^\circ C$  to  $240^\circ C$  (step  $40^\circ C$ )

In the above load-case matrix, only the load cases for which the combination of  $(T_{min}, \Delta T)$  results in a maximum temperature of the cycle not exceeding  $185^\circ$  are retained in the training dataset (with the other data points excluded). The additional 10 load cases used to validate the developed metamodels are listed in Table I.

TABLE I. LOAD-CYCLE CASES FOR METAMODEL VALIDATION

Load	Load Case Ref. Number, #									
	1	2	3	4	5	6	7	8	9	10
$T_{min}$ ( $^\circ C$ )	-35	-35	-35	-35	5	5	5	45	45	85
$\Delta T$ ( $^\circ C$ )	100	140	180	220	60	100	140	60	100	60

Metamodels with the capability for mapping the spatial damage distribution, as obtained with a full-order FE simulation, are constructed for the spatial domain of the solder layer between the chip and the DBC substrate. In this instance, because of the 3D slice nature of the FE model and the negligible damage variation through the slice thickness (Y-direction), the metamodel predictions are needed only for a single X-Z mesh elements cross-section of the solder layer. Without any limitation, metamodel mapping of the spatial distribution of damage in the true 3D local spatial domain can be achieved identically but considering the complete (X, Y, Z) location coordinates. The spatial locations for which the metamodels provide damage predictions are defined by the FE mesh element centre locations in this study (or alternately can be selected as the mesh nodes) for the mesh elements in

the spatial domain of the failure site. The FE mesh of the solder layer X-Z cross section is defined by a mesh grid with the size of  $52 \times 4$  (along X and Z directions respectively), thus resulting in 208 spatial locations with coordinates  $(X, Z)_j$ ,  $j = 1, 2, \dots, 208$ .

The training dataset to derive the MQ metamodel structure parameters for each of these spatial locations is given with the load data points,  $(T_{min}, \Delta T)_i$ ,  $i = 1, 2, \dots, 21$ , in the training dataset. However, for the NN model, the training dataset is modified. The point location parameters are to be directly included as inputs to the NN model structure, thus giving a dataset where each point is a 4-dimensional input vector,  $(T_{min}, \Delta T, X, Z)_i$ ,  $i = 1, 2, \dots, 4368$ , and each such data point is labelled with the corresponding damage value  $\Delta W$  for the load and the location obtained with the FEA. The size of the training dataset for developing an NN model is the product of the load cases (21) and the number of spatial locations (208). Data is normalised in  $[0,1]$  using the actual range of each input parameter in the training dataset. The same procedure for dataset creation is followed with the load-cycle cases for metamodel validation, resulting in 2080 validation data points (10 load cases and 208 spatial locations).

### D. MQ Meta-modelling of Solder Damage

The multi-quadratic (MQ) metamodel structure  $MQ(X)$  [20] is defined as:

$$MQ(X) = \sum_{j=1}^p a_j \sqrt{|X - \bar{X}^j|^2 + h} \quad (2)$$

where  $X \in R^n$  is the model input data point, i.e. the vector of  $n$  input model parameters,  $\bar{X}^j \in R^n$  are the metamodel training points ( $j = 1, \dots, p$ ) with known response values and  $h$  is the so-called shift parameter. The coefficients  $a_j$  are derived by forcing the function in (2) to interpolate (i.e. fit exactly) the given set of response values  $(\bar{X}^j, MQ(\bar{X}^j))$  for the data points deployed in the model development ( $j = 1, \dots, p$ ). This requirement results in solving a linear system of  $p$  equations with the coefficients in the MQ model  $a_j$  ( $j = 1, \dots, p$ ) as unknowns. The optimal value obtained for this problem and the normalised values datasets is  $h = 0.00001$ .

The processing and manipulation of datasets, coding of the MQ model structure and solving the metamodel structure parameters are implemented using MATLAB. The load data points in the training dataset are used to compute the MQ model coefficients, and this is done separately for each spatial location in the representee solder X-Z mesh slice. The entire calculation process is automated for all locations. Following this, a metamodel is derived where the model coefficients are location-dependent and computationally can be easily handled in a matrix form. At the training points, the MQ model predictions have zero error because of the interpolation attribute of the model structure. Hence, the accuracy of the model can be evaluated based on the observed predictive performance for the data points in the validation dataset.

Fig. 5 shows the accuracy of the MQ metamodel, by plotting the actual FE simulation predictions vs. the metamodel predictions for the datapoints in the validation dataset. Both the MSE and the R-squared values show that the MQ offers exceptional accuracy for predicting the damage parameter value  $\Delta W$  at the locations of interest and under varying load conditions. Given the highly non-linear spatial distribution of the damage parameter in the solder layer, as illustrated well with the example in Fig. 4, the MQ

metamodel was able to achieve a very robust performance and exceptional, FE model-matching, accuracy.

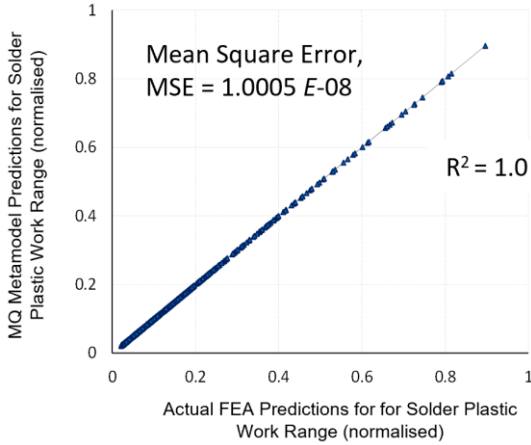


Fig. 5. Predicted values with MQ metamodels vs. actual FEA values of the [0,1]-normalised plastic work range per cycle values  $\Delta W$  obtained for the validation dataset (2080 data points). Each data point in the validation dataset represents a cyclic thermal load condition ( $T_{min}, \Delta T$ ) and a solder layer X-Z cross-section spatial location defined by ( $X, Z$ ).

### E. NN model of Solder Damage

The availability of labelled datasets also suits the deployment of machine learning algorithms in the task of creating regression-type predictive models. As an alternative to the MQ metamodeling approach, the training dataset is used to train a regression Neural Network model structure with four inputs, ( $T_{min}, \Delta T, X, Z$ ), and a single output,  $\Delta W$ . The MATLAB scientific programming environment is used to realise the NN model development, by deploying a hyperparameter optimisation procedure during the training process. A fully connected model structure with 3 hidden layers and size (60, 50, 170), and the rectified linear unit (ReLU) activation function for the fully connected layers of the neural network model, were found to minimise the loss function most effectively.

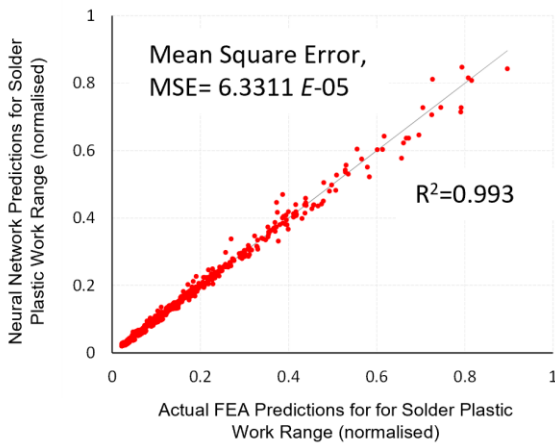


Fig. 6. Predicted values with the Neural Network model vs. actual FEA values of the [0,1]-normalised plastic work range per cycle values  $\Delta W$  obtained for the validation dataset (2080 data points). Each data point in the validation dataset represents a cyclic thermal load condition ( $T_{min}, \Delta T$ ) and a solder layer X-Z cross-section spatial location defined by ( $X, Z$ ).

The accuracy of the NN model is detailed in Fig. 6. Although the actual FEA values of the damage parameter are still predicted reasonably well by the NN model, the accuracy is not as good as with the MQ metamodel. This is attributed

to the explicit increase of the input vector dimension and the highly non-linear relationships of the damage on one side and the load location on the other. An approach that can help improve the accuracy is to generate additional synthetic data for training with the more accurate MQ model, which - as it has been proven - can provide predictions with accuracy like the FE physics-based simulation.

## IV. RESULTS AND DISCUSSIONS

The validation of accuracy for the MQ and NN models detailed in the previous section suggests that both physics-informed MQ metamodel and NN model have very good predictive power, but the MQ metamodel is superior and can deliver predictions that match very closely the actual FEA predictions for the parameter of interest ( $\Delta W$ ). This is an important result because it demonstrates that the metamodeling approach can indeed map physical parameter predictions with highly non-linear spatial distribution (very different magnitudes) over many spatial locations that can represent with a sufficient level of detail the topology of a local failure site. The approach is also scalable, particularly in expanding the number of spatial locations for which the metamodel can provide predictions. This offers opportunities for reasonably detailed and informative mapping of physics-based parameter results in 3-dimensional subdomains of a physical system.

Finite element model and the corresponding MQ metamodel predictions for the  $\Delta W$  at the failure site of interest, for the validation Load Case #7 (Table I, cycle profile defined with  $T_{min} = 5^\circ\text{C}$  and  $\Delta T = 140^\circ\text{C}$ ), are shown in Fig. 7. The contour plots visualise the X-Z plastic work range per cycle distribution in the solder layer.

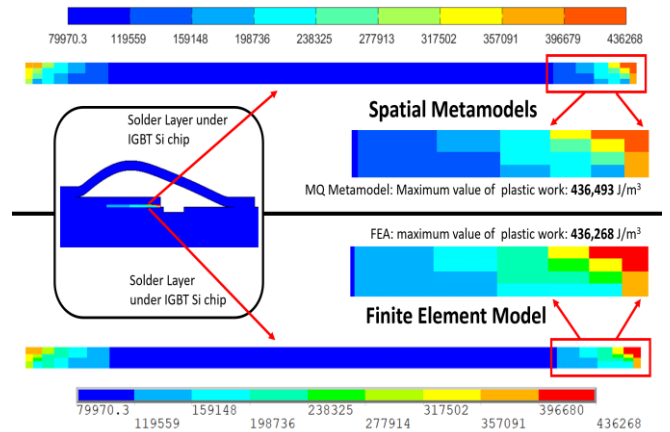


Fig. 7. Damage map of solder die attachment layer (given with the contour plots of the spatial distribution of the inelastic strain energy density, or plastic work, in  $\text{J/m}^3$  accumulated over one temperature cycle) predicted with finite element model (bottom) and MQ metamodels (top). Results are for the validation load case #7 defined  $T_{min} = 5^\circ\text{C}$  and  $\Delta T = 140^\circ\text{C}$ .

The two plots in Fig. 7 use the same legend scale to allow for the direct visual comparison of the presented results. These contour plot results show practically identical predictions of the damage distribution using the same mesh-based resolution mapping. The MQ model predictions match the FE contour plot scale bands across almost all 208 (mesh-defined) spatial locations, except for a few. The relative difference between the maximum plastic work range per cycle values obtained with the FE and MQ metamodel is 0.05%.

A comparative analysis of a characteristic damage value for the solder commonly used with lifetime models, in the form of a volume-weighted average (VWA)  $\Delta W_{ave}$  of the  $\Delta W$  values is demonstrated in Fig. 8. The total volume for the VWA calculation is the solder subdomain where the maximum plastic work concentration is predicted, at the Si chip interface and periphery (the encircled mesh elements in Fig. 4). Statistical measures for the relative errors,  $\varepsilon^{rel}$  in %, of the  $\Delta W_{ave}$  predictions obtained with FEA and MQ metamodel, and FEA and the NN model, across the ten validation load cases are detailed in Table II. The average relative difference in the  $\Delta W_{ave}$  value from the FE and MQ models is 0.09%, and in the case of the FE and the NN models the average relative difference is 0.85%. While in the latter case, the statistical measure still indicates the high accuracy of the NN model, the error is one order of magnitude higher compared with the same error for the MQ metamodel. Across the validation load cases, the largest relative error between the FEA and the MQ metamodel was found with load case #8 ( $\varepsilon_{max}^{rel} = 0.28\%$ ), and for the FEA and NN model this was for load case # 5 ( $\varepsilon_{max}^{rel} = 2.69\%$ ). In conclusion, both MQ metamodel and NN are viable model substitutes of a full-order FEA if calculating the damage characteristic value for cycles to failure predictions using Coffin Manson or Morrow empirical lifetime models.

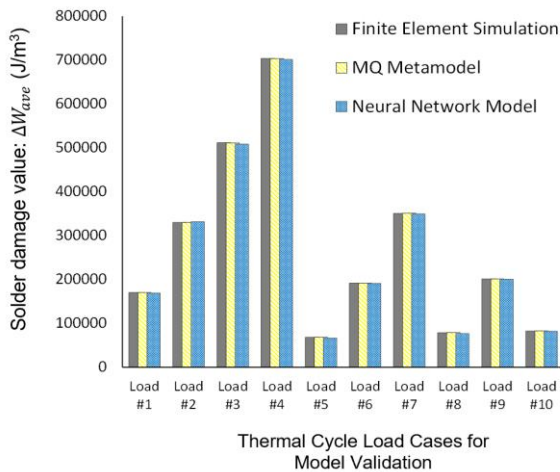


Fig. 8. Solder layer characteristic VWA damage values of plastic work range per cycle  $\Delta W_{ave}$  obtained by high-fidelity non-linear FEA, MQ metamodel, and the unified Neural Network model for the 10 different model validation load cases.

TABLE II. VALIDATION DATASET STATISTICAL MEASURES FOR THE RELATIVE ERROR BETWEEN MQ/NN AND FEA PREDICTIONS FOR  $\Delta W_{ave}$

		Relative error $\varepsilon^{rel}$ (%)			
		$Min$ $\varepsilon_{min}^{rel}$	$Max$ $\varepsilon_{max}^{rel}$	$Mean$ $\varepsilon_{mean}^{rel}$	$Std Dev$
Model	MQ	0.0072	0.282	0.088	0.087
	NN	0.1962	2.692	0.853	0.910

The study shows that the proposed metamodeling modelling approach is very robust and capable of producing model predictions for non-linear damage parameters in PEM assembly materials and their spatial distribution in local failure sites with the accuracy of a full-order finite element simulation. But the metamodels have in addition several important advantages. End-users can evaluate the PEM reliability performance under different load conditions posed

by the application, and manage operational usage, without the need to fully characterise the PEM and to use advanced FE software. Metamodels give predictions in real time, unlike a non-linear FE simulation which can take minutes and hours to complete.

## V. CONCLUSIONS

A methodology for metamodeling is proposed and demonstrated for the problem of predicting the thermal fatigue damage in the solder interconnection layer of an IGBT power electronic module. The main novelties in this work, taking the standard Response Surface Approach for design optimisation and design exploration analysis beyond the current state-of-the-art, are:

- the extension of the physical parameter prediction to the spatial domain, enabling FE-like results for the parameter distribution in a local (failure) site of the physical domain, and this result visualisation. While demonstrated only for the spatial domain, the proposed models can also be tailored to allow the prediction of results in the temporal domain.
- the deployment of a very accurate, highly non-linear multi-quadratic metamodel structure, with a model parameter to tune (optimise) the prediction accuracy;
- MQ model structure that, following validation, can efficiently generate large datasets of synthetic physics-informed physical parameter data for developing more complex and multi-dimensional Neural Network models for predicting highly non-linear behaviour of the response data.

The advantage of the proposed metamodels is that no PEM characterisation data is required to run these models, and the runtime of analysis is only a fraction of the time that the FE simulation takes. The proposed models can be provided by PEM manufacturers as part of the respective module technical datasheets or as supplementary product reliability assessment features, to allow for the component IP protection while enabling the end-users to assess the reliability performance of the PEM under the loads and conditions of their application.

## REFERENCES

- [1] F. Blaabjerg, T. Dragicevic, and Pooya Davar, "Applications of Power Electronics", *Electronics*, vol. 8, 465, 2019.
- [2] H. Wang and F. Blaabjerg, "Power electronics reliability: state of the art and outlook," *IEEE Journal of Emerging and Selected Topics in Power Electronics*, vol. 9, no. 6, pp. 6476-6493, 2021.
- [3] J. O. Gonzalez, *et al.*, "Enabling high reliability power modules: A multidisciplinary task," *Proc. International Symposium on 3D Power Electronics Integration and Manufacturing*, Raleigh, NC, USA, 2016, pp. 1-5, 2016.
- [4] H. Wang *et al.*, "Application-oriented reliability testing of power electronic components and converters," *IEEE Power Electronics Magazine*, vol. 9, no. 4, pp. 22-31, Dec. 2022.
- [5] O. E. Gabriel and D. R. Huitink, "Failure mechanisms driven reliability models for power electronics: a review," *Journal of Electronic Packaging*, vol. 145, no. 2, 020801, Jun 2023.
- [6] K. Ma, H. Wang, and F. Blaabjerg, "New Approaches to Reliability Assessment: Using physics-of-failure for prediction and design in power electronics systems," *IEEE Power Electronics Magazine*, vol. 3, no. 4, pp. 28-41, Dec. 2016.
- [7] P. Rajaguru, H. Lu, and C. Bailey, "Time integration damage model for Sn3.5Ag solder interconnect in Power Electronic Module," *IEEE Transactions on Device and Materials Reliability*, vol. 19, no. 1, pp. 140-148, 2019.

- [8] A. Surendar, V. Samavatian, A. Maselena, *et al.*, "Effect of solder layer thickness on thermo-mechanical reliability of a power electronic system," *Journal of Materials Science: Materials in Electronics*, vol. 29, pp. 15249-15258, 2018.
- [9] Q. Li, *et al.*, "Review of the failure mechanism and methodologies of IGBT bonding wire," *IEEE Transactions on Components, Packaging and Manufacturing Technology*, vol. 13, no. 7, pp. 1045-1057, 2023.
- [10] Q. Huang, C. Peng, S. F.-M. Ellen, W. Zhu, and L. Wang, "A Finite Element Analysis on the reliability of heavy bonding wire for high-power IGBT module," *IEEE Transactions on Components, Packaging and Manufacturing Technology*, vol. 11, no. 2, pp. 212-221, 2021.
- [11] J. Johansson, I. Belov, E. Johnson, and P. Leisner, "A computational method for evaluating the damage in a solder joint of an electronic package subjected to thermal loads," *Engineering Computations*, vol. 31, no. 3, pp. 467-489, 2014.
- [12] M. Tauscher, T. Merk, A. Adsule, A. Linnemann, and J. Wilde, "Surrogate modeling for creep strain-based fatigue prediction of a Ball Grid Array component," *ASME Journal of Electronic Packaging*, vol. 146, no. 1, 011003, 2023.
- [13] P. Rajaguru, S. Stoyanov, H. Lu, and C. Bailey, "Application of Kriging and radial basis function for reliability optimization in power modules," *Journal of Electronic Packaging*, vol. 135, no. 2, 021009, June 2013.
- [14] B. Ji, X. Song, E. Sciberras, W. Cao, Y. Hu, and V. Pickert, "Multiobjective design optimization of IGBT power modules considering power cycling and thermal cycling," *IEEE Transactions on Power Electronics*, vol. 30, no. 5, pp. 2493-2504, May 2015.
- [15] R. H. Myers, D. C. Montgomery, and C. M. Anderson-Cook, *Response Surface Methodology: Process and Product Optimization Using Designed Experiments*, Wiley, 4th ed., 2016.
- [16] M. Ciappa, "Lifetime modeling and prediction of power devices," *Proc. 5th International Conference on Integrated Power Systems (CIPS)*, 2008, pp. 1-9.
- [17] G. Riedel, R. Schmidt, C. Liu, H. Beyer, and I. Alapera, "Reliability of large area solder joints within IGBT modules: Numerical modelling and experimental results," *Proc. 7th International Conference on Integrated Power Systems (CIPS)*, 2012, pp. 288-298.
- [18] G. Z. Wang., Z. N. Cheng, K. Becker, and J. Wilde, "Applying Anand model to represent the viscoplastic deformation behavior of solder alloys," *ASME Journal of Electronic Packaging*, vol. 123, no. 3, pp. 247-253, 2001.
- [19] E. Milke and T. Mueller, "High temperature behaviour and reliability of Al-Ribbon for automotive applications," *Proc. 2nd Electronics System-Integration Technology Conference*, pp. 417-422, 2008.
- [20] R. L. Hardy, "Multiquadratic equations of topography and other irregular surfaces," *Journal of Geophysical Research*, vol. 76, issue 8, pp. 1905-1915, 1971.